HHS Public Access

Author manuscript

Langmuir. Author manuscript; available in PMC 2020 November 03.

Published in final edited form as:

Langmuir. 2019 July 09; 35(27): 9071–9083. doi:10.1021/acs.langmuir.9b01227.

Responses of *Acinetobacter baumannii* Bound and Loose Extracellular Polymeric Substances to Hyperosmotic Agents Combined with or without Tobramycin: An Atomic Force Microscopy Study

Muhammedin Deliorman[†], **F. Pinar Gordesli Duatepe**[‡], **Emily K. Davenport**[§], **Boel A. Fransson**[‖], **Douglas R. Call**[⊥], **Haluk Beyenal**[§], **Nehal I. Abu-Lail**[*,#]

[†]Division of Engineering, New York University Abu Dhabi, P.O. Box 129188, Abu Dhabi, UAE

[‡]Faculty of Engineering, Izmir University of Economics, 35330 Izmir, Turkey

[§]Gene and Linda Voiland School of Chemical Engineering and Bioengineering, Washington State University, 99164 Pullman, Washington, United States

[‖]Department of Veterinary Clinical Sciences, Washington State University, 99164 Pullman, Washington, United States

[⊥]Paul G. Allen School for Global Animal Health, Washington State University, 99164 Pullman, Washington, United States

[#]Department of Biomedical Engineering, University of Texas at San Antonio, 78249 San Antonio, Texas, United States

Abstract

In this work, contributions of extracellular polymeric substances (EPS) to the nanoscale mechanisms through which the multidrug-resistant *Acinetobacter baumannii* responds to antimicrobial and hyperosmotic treatments were investigated by atomic force microscopy. Specifically, the adhesion strengths to a control surface of silicon nitride (Si_3N_4) and the lengths of bacterial surface biopolymers of bound and loose EPS extracted from *A. baumannii* biofilms were quantified after individual or synergistic treatments with hyperosmotic agents (NaCl and maltodextrin) and an antibiotic (tobramycin). In the absence of any treatment, the loose EPS were significantly longer in length and higher in adhesion to Si_3N_4 than the bound EPS. When used individually, the hyperosmotic agents and tobramycin collapsed the *A. baumannii* bound and loose EPS. The combined treatment of maltodextrin with tobramycin collapsed only the loose EPS and did not alter the adhesion of both bound and loose EPS to Si_3N_4. In addition, the combined

[*]**Corresponding Author:** nehal.abu-lail@utsa.edu. Phone: +1 210 458 8131.

The authors declare no competing financial interest.

ASSOCIATED CONTENT

Supporting Information

The Supporting Information is available free of charge on the ACS Publications website at DOI: 10.1021/acs.langmuir.9b01227. Percentages of curves displaying multiple adhesion events acquired on *A. baumannii* bound and loose EPS under a number of tested conditions, detachment forces versus polymer extension plots for *A. baumannii* bound and loose EPS after NaCl treatments, detachment forces versus polymer extension plots for *A. baumannii* bound and loose EPS after tobramycin treatments, and mass concentrations of bound and loose EPS extracted from the biofilm suspensions of *A. baumannii* (PDF)

treatment was not as effective in collapsing the EPS molecules as when tobramycin was applied alone. Finally, the effects of treatments were dose-dependent. Altogether, our findings suggest that a sequential treatment could be effective in treating *A. baumannii* biofilms, in which a hyperosmotic agent is used first to collapse the EPS and limit the diffusion of nutrients into the biofilm, followed by the use of an antibiotic to kill the bacterial cells that escape from the biofilm because of starvation.

Graphical Abstract

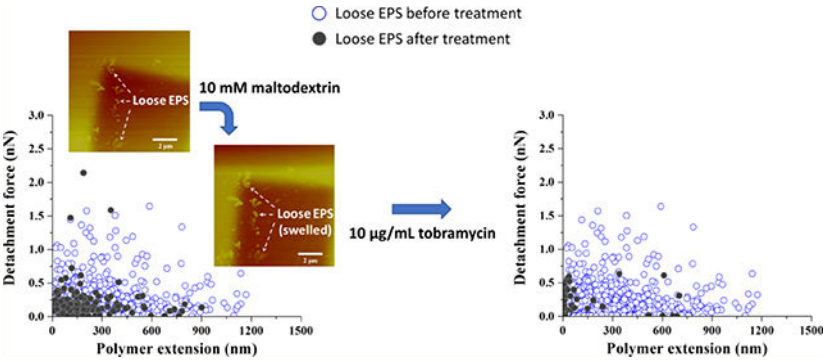

INTRODUCTION

Bacterial biofilm infections, ranging from minor to life-threatening, are common and affect people of all ages around the globe.[1] Most pathogens causing these infections, including *Acinetobacter baumannii, Staphylococcus aureus*, and *Pseudomonas aeruginosa*, are becoming increasingly resistant to a range of commonly available antibiotics, which results in a greater challenge in the treatment of the patients. Among them, opportunistic *A. baumannii* has raised great concerns in health care settings worldwide as a frequent cause of wound, urinary tract, and blood stream infections, to name a few.[2,3] *A. baumannii* ranks among the most important nosocomial pathogens, and numerous studies have reported the presence of multidrug resistant (MDR) *A. baumannii* in hospitals.[3–6]

A. baumannii establishes an infection first by adhering to the host surface and then by colonizing it.[1,7,8] The adhered bacteria produce extracellular polymeric substances (EPS) to form biofilms on the surface, resulting in a natural protective shield for the bacteria against treatment options with antibiotics, leading to chronic infections.[9–11] The production of EPS by bacteria during biofilm formation is thought to be a key platform conveying the biofilm resistance to antibiotics.[12] When maturing, the bacterial biofilms connected with EPS provide a protection for the population of cells within the biofilm from the antibiotics because of mass transport limitations.[13] This population of cells is called persister cells.[14] Persisters are resistant to antibiotics applied to biofilms at a concentration that is 20 times the minimum inhibitory concentration required to kill bacteria in a planktonic culture.[15,16] As such, EPS adhesion to surfaces leads to thicker biofilms that protect the persister cells from antibiotics, resulting in resistance to antibiotics in the bacterial population. The number of these cells increase exponentially in each cycle of proliferation.

EPS are comprised of polysaccharides, proteins, glycoproteins, lipids, and nucleic acids, and their composition varies depending on the bacterial species, physiological status of the cells, and a wide range of environmental factors.[17] Hence, the complexity of EPS delays or prevents—by diffusion limitation and/or interactions—the penetration of antimicrobial agents, antibiotics, and other biocides to the full depth of a biofilm so they cannot reach the bacteria.[18,19] For example, in terms of diffusion limitations, a set of investigations suggested that younger and thinner biofilms are more susceptible to diffusion of biocides than the older and thicker ones.[20] In terms of interactions, it was reported that glycocalyx, a membrane-bound network of polyanionic EPS biopolymers, inactivates the effect of biocides by exchanging ions,[21] whereas in terms of electrostatic interactions, it was shown that alginate, the major oligosaccharide component of EPS in Pseudomonas biofilms, prevents biocides and aminoglycosides such as tobramycin and gentamicin from penetrating into the biofilm by binding to them through opposite charges.[22] Other forces that can play a factor in how bacterial EPS interact with external molecules such as antibiotics or hyperosmotic agents include van der Waals forces, hydrogen bonds, and acid–base interactions.[23,24]

To date, two distinct types of EPS (bound and loose) have been classified based on well-established EPS extraction protocols.[25–28] Among them, bound EPS is a protein-rich layer tightly bound to the cell wall of the bacteria. In comparison, loose EPS is a relatively thicker layer that only coats the bacterial outer cell surface and imparts sticky consistent growth on a solid medium or an increased viscosity in a liquid environment.[29] Both types of EPS have definite forms and boundaries.[27] Despite their indisputable importance to the process of biofilm formation, the relevance of bound and loose EPS toward enabling the bacteria to resist antibiotics or to adhere to surfaces remains poorly understood.

Because of their abilities to resist antibiotics, alternative strategies have been investigated in the treatment of chronic infections caused by MDR bacteria. Among them, the use of hyperosmotic agents has been proposed as a promising strategy in the treatment of chronic wounds. Studies showed that hyperosmosis from high NaCl concentrations reduces the biomass and viability of *A. baumannii*,[30] *Enterococcus faecalis*,[31] *P. aeruginosa*,[31] and *Streptococcus mutans*[32] biofilms in vitro. For wounds, however, high NaCl concentrations could be problematic and may impair healing. For example, it was reported that exposure of mammalian cells to concentrations of >160 mM NaCl causes strand breakage in their DNA and results in repair delays.[33] Alternatively, a nontoxic common sweetener, maltodextrin, which is mainly composed of polysaccharides, can act as a hyperosmotic agent against biofilm cells and thus be effective in the treatments.[34,35] It was only recently demonstrated that combining maltodextrin with common antibiotics, such as vancomycin and tobramycin, improves the antibiotic efficacy against *S. aureus* biofilms[36] and results in a reduced number of *A. baumannii* biofilm cell counts,[37] respectively. However, the authors in these studies noted that when used in relatively higher concentrations (greater than 20 mM), maltodextrin results in slowing the diffusion of the antibiotics, thus reducing their overall efficacy against the infection. Although the use of hyperosmotic agents combined with antibiotics seems to be a promising strategy to combat bacterial biofilms, further research is needed to elucidate the mechanisms by which biofilms and their EPS constituents provide protective responses against such combined treatments.

The use of atomic force microscopy (AFM) in assessing the nanostructure and mechanical properties of EPS secreted by different microorganisms is greatly advanced. AFM offers an ideal platform for evaluating the adhesion between two surfaces that are in contact with each other.[38,39] Furthermore, AFM has been extensively used to characterize the elastic properties of single macromolecules, such as proteins,[40] nucleic acids,[41] polysaccharides,[42] and bacterial surface molecules.[43,44] The latter has been mainly achieved by measuring the adhesion forces between bacterial cells immobilized onto different substrates, such as glass or polystyrene, and AFM cantilevers. AFM also provides quantitative information on the heterogeneity, adhesion capacity, and mechanics of EPS in real time and in the presence of liquid media such as hyperosmotic agents or antibiotics.[44–46]

Although it is acknowledged that the bound and loose EPS act as diffusion barriers to protect bacteria from antibiotics by preventing their penetration into the biofilm,[26] knowledge about the strength and nature of the adhesive forces between bound and loose EPS and the surfaces after exposure to hyperosmotic compounds combined with or without antibiotics is in its infancy. AFM can easily serve as a tool to measure these adhesion forces along with conformational properties of the EPS in the presence of such compounds.[23,24,44] To our knowledge, no investigation has been reported on the use of AFM to determine explicitly how bound and loose EPS respond to hyperosmotic agents or antibiotics by evaluating their adhesion strengths and lengths, which is what this study focuses on. The lack of such knowledge impedes the abilities of researchers to design effective combined treatments to control the MDR *A. baumannii* infections.

Here, AFM was utilized to investigate how bound and loose EPS change their adhesion strengths and conformational properties when subjected to different concentrations of NaCl (control), maltodextrin, tobramycin, and combined maltodextrin and tobramycin solutions in vitro. Implications of how EPS respond to combined or individual treatments on bacterial mechanisms of MDR bacteria are also discussed.

EXPERIMENTAL METHODS

Cell Culture and EPS Extraction.

A. baumannii (ATCC BAA-1605) was used in all experiments. The strain was isolated from the sputums of military personnel returning from Afghanistan and entering Canadian hospitals on June 30, 2006. This strain is resistant to ceftazidime, gentamicin, ticarcillin, piperacillin, aztreonam, cefepime, ciprofloxacin, imipenem, and meropenem and sensitive to amikacin and tobramycin.[47,48] EPS components were extracted from *A. baumannii* biofilms ($n = 8$) as described in the literature.[26] Briefly, each biofilm was grown in a membrane bioreactor for 3 days. Then, the membrane was removed and rinsed three times with 3 mL 0.9% NaCl to suspend the biofilm. Afterward, the biofilm suspension was centrifuged for 5 min at 5000g, and the EPS in the supernatant was collected as loose EPS. Pelleted cells were then resuspended in 1 mL 0.9% NaCl solution and centrifuged for 5 min at 5000g, and the EPS in the supernatant was added to the loose EPS. Finally, the pelleted cells were resuspended in 1 mL 0.9% NaCl, heated to 80 °C for 8 min, and centrifuged for 15 min at 15 000g and 4 °C, and the EPS in the supernatant was collected as bound EPS. Both bound and loose EPS were sterilized using 0.45 μm pore-sized filters to remove the remaining cells in

the supernatant, quantified for their mean mass concentrations[49] (i.e., the actual mass of bound and loose EPS in μg per volume of cell culture in mL, Table S1), labeled as untreated, and stored at −20 °C as stock solution for future use.

Even though we are differentiating the EPS fractions into bound EPS and loose EPS, there is no complete guarantee that either fraction will not have proteins resulting from cell lysis such as extracellular proteins and outer membrane proteins. However, since the actively secreted extracellular proteins are not tightly associated with the bacterial cell surface, they are expected to be present more in the loose EPS fraction. On the other hand, bound EPS, which are tightly associated with the bacterial cell surface, are expected to contain more outer membrane proteins than the loose EPS. This was indeed the case when the bound and loose EPS from *Shewanella* sp. HRCR-1 biofilms were characterized using infrared spectroscopy and proteomics.[25] Their results indicated that most of the extracellular proteins (5 out of 7) were abundant in the loose EPS, whereas the majority of the outer membrane proteins (27 out of 51) were abundant in the bound EPS. Therefore, based on their findings, it is expected that the bound and loose EPS of *A. baumannii* biofilms will contain proteins from cell lysis. However, the extent to which these proteins affect the content of our EPS fractions is minimal. Literature studies indicate that very low carbohydrate-to-protein w/w ratios such as <0.11[50] are indicative of contamination of EPS by lysed cell materials. Here, the ratios of carbohydrates to proteins in the bound and loose EPS samples in our study were determined as 0.21 and 0.16, respectively (Table S1), which are in good agreement with the ratios for biofilm EPS reported by others.[25,50,51] Hence, our results suggest that there is no significant contamination of lysed cell materials in the EPS samples used in the presented work.

Substrate Cleaning, Patterning, and Modification.

Silicon wafers were cut into ~1 × 1 cm^2 specimens, ultrasonically cleaned in deionized water and 70% ethanol for 3 min, and then immersed in piranha solution (95% H_2SO_4/35% H_2O_2, 4:1 in volume) for 30 min at 25 °C. Afterward, the specimens were rinsed several times with water and ethanol and dried under a nitrogen stream. The freshly cleaned wafers were then etched using a microfocused $^{69}Ga^+$ beam of a triple focusing time-of-flight secondary ion mass spectrometry (ToF-SIMS) system (PHI-Evans) to create patterned areas on silicon surfaces, each with a size of 10 × 10 μm^2. The carefully adjusted sputter time was 10 s, so that ~2 nm layer of the substrate surface would be removed.[52] Thereafter, the etched silicon wafers were immersed in a solution of 0.5% (v/v) 3-aminopropyltri-ethoxysilane (APTES) in dry toluene for 45 min at 25 °C. After silanization, the substrates were sonicated in ethanol for 5 min, dried with nitrogen, and placed in 100 °C oven for 30 min for APTES annealing.[52] This way, a monolayer (~0.8 nm) of uniformly distributed (~1:1 ratio) reactive amine and protonated nitrogen groups were created on the surfaces of patterned areas.[52] Finally, silicon chips were kept in phosphate-buffered saline (PBS) at 25 °C for further immobilization of bound and loose EPS as described below.

EPS Immobilization.

Extracted *A. baumannii* bound and loose EPS were allowed to immobilize on predefined patterned areas of silanized silicon substrates by pipetting ~200 μL of the stock solution for

60 min at 25 °C. After incubation, the loosely attached loose EPS were removed from the surface by washing the samples with PBS. This was to ensure that only firmly attached loose EPS remain on the substrate so that they can withstand the detachment forces exerted by the AFM tip. Immediately after, the samples were analyzed with AFM under different treatments.

AFM Force Measurements.

All AFM force measurements of bound and loose EPS were collected in PBS at 25 °C using a Nanoscope III system (Bruker) equipped with a Quadrexed module that allows operations in MultiMode and silicon nitride (Si_3N_4) AFM cantilevers (Bruker) having a nominal spring constant of ~0.06 N/m. Here, unmodified Si_3N_4 AFM cantilevers were used to measure the adhesion strengths and conformational properties of the bound and loose EPS, as a good reference substrate with controlled chemical properties was needed to compare the EPS responses under different treatments.

Prior to each measurement, the thermal tune method[53] was used to experimentally obtain the cantilever spring constant, and a clean silicon surface was used to calibrate the sensitivity of the photodiode. The cantilever approach and retract velocities were set to ~3 μm/s. Steel pucks (Ted Pella), to which silicon chips were mounted on, were covered with hydrophobic Teflon membranes to serve as a liquid barrier. Prior to each set of experiment, the AFM tips were cleaned with ultraviolet/ozone to ensure that the tip surfaces are free of contaminants. The adhesion force measurements were performed in the force-volume (FV) mode using a standard fluid cell (Bruker), in which the approach-retraction process was repeated over 10 × 10 μm^2 predefined areas of the silicon surface at a resolution of 32 × 32 pixels per FV image and at 20 min acquisition time. The trigger force was set to ~0.5 nN. The applied force–displacement curves on all pixels in the FV image were converted into force–separation profiles and analyzed with a home-written software[54,55] to provide information on the strength of the adhesion forces as well as the pull-off distances (PDs) as they attach to the cantilever and stretch upon retraction before their final detachment.

Representative FV image and force–separation curve associated with *A. baumannii* loose EPS are shown in Figure 1a,b, respectively. At each pixel in the FV image, the quantitative analysis of adhesion forces between the Si_3N_4 AFM cantilever surface and the EPS was performed by first identifying the local minima on the retraction curve (e.g., representative peaks 1 and 2 in Figure 1b). Subsequently, the length of the EPS molecules was obtained from their PDs (detachment), assuming that the molecules are sequentially detached from the cantilever surface.[24,56] Adhesion events below 0.1 nN cutoff force (e.g., the representative peak marked with * in Figure 1b) were regarded as noise and excluded from the analysis. As a result, histograms (number of bins = 25) describing the distributions of total adhesion forces and the corresponding PDs were constructed for both bound and loose EPS under the investigated conditions, and the number of adhesion events per force profiles were quantified (Figure S1). Origin software (OriginLab) was used to evaluate the arithmetic mean and standard deviations of the histograms (Table 1). Finally, for both bound and loose EPS, maximum adhesion force values (e.g., peak 1 in Figure 1b) were assigned to each pixel in the adhesion maps (Figure 2a,b), whereas the corresponding PDs were assigned to each

pixel in the PD maps (Figure 2c,d), except for force profiles with an unclear approach and/or retraction curve. In the latter cases, their adhesion and PD values were set to 0 at corresponding pixels in the maps.

Statistical Analysis.

Statistical analysis was performed with OriginPro software using two-way analysis of variance to evaluate the differences between the adhesion forces or PDs of bound and loose EPS investigated under different conditions. A P-value of <0.05 was considered statistically significant.

RESULTS AND DISCUSSION

Adhesion and Pull-Off Characteristics of Untreated Bound and Loose EPS.

Representative adhesion force and PD maps associated with untreated *A. baumannii* bound and loose EPS are shown in Figure 2. The variations in the adhesion forces and PDs for bound EPS (up to 0.8 nN and 184 nm) and loose EPS (up to 1.3 nN and 1140 nm) indicated the heterogeneous EPS characteristics. Overall, the mean adhesion forces of bound and loose EPS to Si_3N_4 were 0.144 ± 0.002 and 0.177 ± 0.002 nN, respectively (Table 1). The corresponding mean PDs of loose EPS (218.0 ± 9.2 nm) were significantly longer than for the bound EPS (106.4 ± 4.7 nm) ($P < 0.05$). The longer extensions of loose EPS biopolymers can be due to proteins' multiple unfolding events[40] and extension and stretching of long polysaccharides[42,57] as well as stretching of glycoproteins.[58,59]

The above results suggest that in the absence of any treatment, the EPS adhesion strength is directly proportional to the length of EPS biopolymers, irrespective of being bound or loose EPS. This was verified when the detachment forces of untreated EPS biopolymers from the AFM cantilever surface were plotted as a function of their extensions (Figure S2). The data were scattered in the plots, however, with a positive trend in the 0–300 nm region, indicating that as the length of polymers increases, higher forces are required to stretch or unravel the polymer chains. Previously, in a number of studies involving colistin-resistant *A. baumannii*[60] and *Listeria monocytogenes*[61] planktonic cells, it was reported that longer molecules adhere more strongly to the Si_3N_4 AFM cantilever surface as a result of the entropic configurations that favor their attachment to the Si_3N_4 surface compared to shorter molecules.[62] Figure 3a shows the distribution of the adhesion forces collected between untreated bound and loose EPS and the Si_3N_4 AFM cantilever surface in PBS. When compared, loose EPS molecules were more heterogeneous than bound EPS molecules, as evident from the larger span of their adhesion forces (Figures 3a and 2a,b). The heterogeneity was linked to the ~2-fold higher number of adhesion events recorded for the loose EPS molecules compared to the bound ones (Table 1). In addition, the percentage of several peaks per force profiles (Figure S1) was ~3-fold higher for loose EPS (35%) compared to bound EPS (13%). In the literature, observing several peaks per force curve (i.e., higher adhesion and higher heterogeneity) was suggested to reflect higher density of molecules on the surface[63,64] as well as the possibility of the AFM cantilever contacting the EPS molecule at more than one location.[65]

To investigate the heterogeneities discussed above, the total and individual bound and loose EPS mass concentrations of proteins and carbohydrates were compared (Table S1). When all biomass contents (proteins and carbohydrates) were summed, the bound EPS were characterized by 1.6-fold biomass compared to the loose EPS (Table S1). When investigated separately, the bound EPS had ~1.5- and 2-fold more proteins and carbohydrates, respectively, compared to the loose EPS (Table S1). When individually assessed, the ratios of proteins to carbohydrates were 6.4 and 4.7 for the loose and bound EPS, respectively (Table S1). As such, it is our expectation that the higher content of proteins in either fraction will contribute more toward the adhesion forces measured with AFM, heterogeneities in adhesion, and the number of observed peaks than the carbohydrates. Because AFM is just a physical tool, it is incapable of detailing the chemical structures of the interacting EPS molecules to feature which contributes to adhesion to the AFM Si_3N_4 cantilever, more proteins or carbohydrates. Without knowing the chemical structures of the abundant proteins and carbohydrates in an EPS fraction, it is hard to discern the roles of carbohydrates and proteins on the estimated PDs and heterogeneities observed in the adhesion data. For example, we cannot conclude that because bound EPS has more proteins than loose EPS, it should have longer PDs. The proteins present in the bound EPS could be aggregates that do not unfold to long distances while those present in the loose EPS can unfold to long distances. Similarly, we cannot conclude that because the bound EPS has more biomass in general than the loose EPS, it will be more heterogeneous. The biomass of the bound EPS may all be composed of similar molecules and as such may not contribute to heterogeneous force data. Therefore, in the future, spectral microscopy of the structure and composition of the bound and loose EPS fractions can help elucidate which molecules are abundant in each EPS fraction and, as such, capable of contributing to the heterogeneities observed.[44] Combining physical tools capable of quantifying adhesion and conformations of EPS, such as AFM, with spectral microscopy tools such as Raman microscopy,[66] Fourier transform infrared (FTIR) spectroscopy, and attenuated total reflection–FTIR microscopy[67,68] capable of resolving the spatial chemical structures of the EPS molecules will enable the researcher to elucidate the relationships between the structure and functions of variable EPS components.

NaCl Treatment.

In this work, NaCl was used as a control hyperosmotic agent. Figure 4a,b shows the distributions of adhesion forces collected for bound and loose EPS treated with 1 and 2 M NaCl, respectively. In comparison to when no treatment was used, in the presence of 1 M NaCl, the adhesion forces of bound EPS significantly increased by 54%, whereas those of loose EPS significantly reduced by 27% ($P < 0.05$, Table 1). Increasing the ionic strength of NaCl to 2 M further significantly increased the adhesion forces of bound EPS by 55% ($P < 0.05$), whereas the adhesion strengths of the loose EPS remained relatively unchanged (Table 1). These findings suggest that 1 M NaCl was enough to suppress the adhesion of loose EPS to ionic strength. However, at the bound EPS level, higher concentrations of NaCl (>2 M) were still needed to induce stress and modulate the bacterial adhesion further. Figure 4a,b also indicates that bound EPS was more heterogeneous than loose EPS under the NaCl concentrations investigated. This heterogeneity in part can explain the stronger adhesion (Table 1) and the higher number of adhesion events observed for the bound EPS under NaCl

(Figure S1). Furthermore, differences in the composition of the EPS for bound and loose fractions can also be responsible for the differences in how they respond to NaCl treatment. As can be seen from Table S1, the bound EPS had 1.4-fold DNA, 2.1-fold carbohydrates, and 1.52-fold proteins than the loose EPS. Even though we have no chemical information on the makeup of these molecules, we still expect that when fractions have such differences between them in composition, they will respond differently to NaCl treatment. Larger variations as such will enable more molecules to be available for interactions with a given substrate. Heterogeneities in EPS are assumed to be the result of variations in the composition, charge, hydrophobicity, and side group chemistry as well as conformations of the molecules making up the matrix.[69] Previously, we showed that when heterogeneities in the elasticities or PDs of bacterial surface molecules increased, the adhesion forces increased as well.[70,71] Heterogeneities were quantified in terms of standard deviations and width of histograms representing the properties above.

The decrease in the loose EPS adhesion strength or the increase in the adhesion of the bound EPS with the introduction of NaCl (Table 1) can be partially explained by the contributions of electrostatic repulsions to the overall interactions acting between the charges of the EPS molecules and the negatively charged Si_3N_4 AFM cantilever surface in PBS (pH = 7.4). Previously, we have shown that as the concentration of NaCl changed from that of pure water to 1 M, two transitions that can be explained by electrostatic charges were observed in the measured nanoscale adhesion of *Pseudomonas putida* KT2442 to silicon nitride.[72] First, at a relatively small NaCl solution concentration, in comparison to the concentration of ions present on the biomolecules of *P. putida* KT2442, partial screening of charges on the biomolecules of the bacterial surface only takes place.[65] As such, the remaining charges of ions of the biomolecules contribute to the repulsive electrostatic forces and lead to decreased adhesion. We think that a similar scenario can explain the decreased adhesion observed for the loose EPS in the presence of NaCl. Second, if the concentration of NaCl in the solution is high enough to screen all ion charges present on the bacterial surface molecules, the role of electrostatic repulsion diminishes, resulting in increased adhesion.[72] This second transition can potentially explain the higher adhesion observed for the bound EPS. Our findings, as such, suggest that when 1 M NaCl was used for both bound and loose EPS, the concentration of ions in solution was sufficient to neutralize the bound EPS charges, at least partially, but was not sufficient to neutralize the loose EPS charges. In the future, testing the hypothesis that loose EPS are more charged than bound EPS can confirm the speculation above about the role of electrostatic charges in dominating the adhesion forces measured between EPS and silicon nitride.

When the PDs were compared (Table 1, Figure 4c,d), it was clear that introducing NaCl collapsed both bound and loose EPS molecules (Figure S2). Introducing 1 M NaCl to the medium significantly reduced the PDs of bound and loose EPS by 75 and 90%, respectively ($P < 0.05$). Introducing 2 M NaCl to the medium did not induce any further reductions in the bound EPS pull-offs but further increased the loose EPS pull-offs by 67%. The adhesion force and pull-off histograms of bound and loose EPS were slightly narrower at 1 M NaCl compared to those measured in 2 M NaCl (Figure 4). This indicates that the ionic strength of 2 M NaCl resulted in a mild heterogeneity in both bound and loose EPS compared to 1 M NaCl, which was also reflected by the increment increase of their multiple adhesion events

(Figure S1). In addition, when 2 M NaCl was used, the mean length of the polymer extensions of bound EPS did not change compared to 1 M NaCl-treated ones (Figure S2a,b). However, their overall adhesion forces significantly increased (Table 1). As for the loose EPS, their mean adhesion forces did not change (Table 1), whereas their mean length of polymer extensions significantly increased (Figure S2a,b). These results further indicate that the collapse of bound and loose EPS was a result of a change in their conformational properties (Figure S2).

Introducing NaCl to the medium can affect the bacterial adhesion via several means. First, it can act as a "charge screener" resulting in a neutralized bacterial charge surface and thus affecting the electrostatic interactions that modulate the adhesion processes.[23,64] Second, the imbalance between the concentration of NaCl in PBS solution and the concentration of ions in the bacterial cytoplasm can induce certain osmotic and excluded volume effects that affect the steric repulsions measured between the EPS molecules and the Si_3N_4 AFM cantilever surface.[64] Third, the presence of NaCl can manipulate the conformations of the EPS molecules.[23] Most often, it results in molecular collapse, and as such, certain chemical groups become hidden and play no more role in controlling bacterial interactions with the surfaces. With the above in mind, and even though we saw effects of NaCl introduction on EPS adhesion to Si_3N_4, the mechanisms by which NaCl affected the bound and loose EPS were quite different.

When the bound EPS were compared, upon increased ionic strength from 1 to 2 M NaCl, the frequency of several adhesion peaks (Figure S1) and the PDs (Figure 1b)—which are proportional to the lengths of EPS—remained relatively unchanged. This indicates that bound EPS preserved their heterogeneity after further NaCl treatment. Further, the observed higher adhesion strengths can possibly contribute to charge screening and control of steric repulsion rather to conformational mechanical effects of the EPS molecules. Finally, the loose EPS were slightly more extended in 2 M NaCl than in 1 M NaCl concentrations (Table 1, Figure S2c,d), indicating that for the outer layer of the bacterial biofilm, NaCl acts mainly on the surface mechanics of EPS and manipulates the conformation of the molecules rather than manipulating their composition.

Maltodextrin Treatment.

When bound EPS were investigated, the adhesion forces to Si_3N_4 remained unchanged upon increasing the maltodextrin concentrations from 1 and 10 mM. Yet, these concentrations resulted in ~20% significant increase in the adhesion forces of the bound EPS to Si_3N_4 compared to untreated ones ($P < 0.05$, Table 1). When the loose EPS were considered, 1 mM maltodextrin significantly decreased the adhesion forces by 18% on average as compared to untreated ones ($P < 0.05$, Table 1), whereas 10 mM maltodextrin significantly increased these forces by ~9% ($P < 0.05$, Table 1). Histograms of adhesion forces and PDs for both bound and loose EPS were broader after 10 mM maltodextrin treatment as compared to 1 mM maltodextrin (Figure 5a,b). The increase in the frequency of the adhesion events as a function of maltodextrin treatment of bound EPS suggested that they are more heterogeneous in nature compared to loose EPS (Figure S1).

At 1 mM maltodextrin, the PDs for bound and loose EPS were more localized with the majority of the population located at ~40 nm, whereas at 10 mM maltodextrin, they were largely spread up to 300 nm (Figure 5c,d). Compared to untreated EPS, introducing 1 mM maltodextrin caused a collapse in the PDs of both bound and loose EPS approximately by 60 and 80%, respectively, which was expected due to osmotic pressure differences. As such, the EPS matrix is expected to provide a highly hydrated environment that dries more slowly than its surroundings.[73] Hyperosmotic agents such as NaCl and maltodextrin create osmotic pressure differences within the biofilm fluid, which will drive water out of the EPS matrix, leading to collapse in the EPS molecules. Interestingly, however, introducing maltodextrin at 10 mM concentration significantly extended the length of the bound and loose EPS molecules, compared to 1 mM maltodextrin-treated and untreated bound EPS ($P < 0.05$, Table 1), but resulted in a significant collapse of loose EPS compared to untreated ones (49% decrease in the PD, $P < 0.05$).

A previous study[74] of the in silico analysis of *A. baumannii* biofilm-associated protein (Bap) sequence revealed that *A. baumannii* Bap contains homologous domains to the polycystic kidney disease (PKD) domain and the concanavalin A-like lectin/glucanase domain. The PKD domain has been implicated in protein–protein interactions, whereas the presence of the concanavalin A-like lectin/glucanase domain suggests possible protein–carbohydrate interactions. Given that maltodextrin can be used as a carbon source by *A. baumannii*,[37] biofilm-associated proteins (Bap and Bap-like proteins) and extracellular carbohydrate-binding proteins (lectins) as well as periplasmic and membrane proteins have been found in the EPS of Gram-negative bacteria.[74–76] The possible formation of protein–carbohydrate complexes and/or protein–maltodextrin conjugates (such as maltodextrin binding protein–maltodextrin conjugate) might be the reason for the observed swollen EPS molecules (Figure 6) at 10 mM maltodextrin concentration. It is clear that the swelling of EPS molecules was not due to water retention. It was possibly arising from the adsorption of the large mass compound maltodextrin (2555 Da)[37] on the EPS surfaces. Further proteomic analyses of the EPS proteins of *A. baumannii* and measurements of equilibrium binding constants of probable EPS protein–carbohydrate complexes may elucidate the observed phenomenon.

Tobramycin Treatment.

When compared to untreated EPS, introducing a solution of tobramycin at 2 μg/mL concentration did not have any effect on the adhesion forces of bound EPS but decreased those of loose EPS (Table 1). At higher tobramycin concentration (10 μg/mL), however, the adhesion forces of both bound and loose EPS significantly increased by ~90 and ~16%, respectively, as compared to untreated ones ($P < 0.05$). The distributions of adhesion forces of bound and loose EPS at 2 μg/mL were narrow and homogeneous, whereas at 10 μg/mL, they were broad and heterogeneous (Figure 7a,b). The PDs of bound and loose EPS extended for up to 300 nm at both tobramycin concentrations, with the majority of the molecules located below 30 nm (Table 1, Figure 7c,d).

Previously, Davenport et al.[26] investigated on the macroscale whether the protective mechanism of *A. baumannii* EPS against tobramycin was due to adsorption of tobramycin to

charged binding sites of the EPS. For this purpose, they first harvested EPS from mature biofilms of *A. baumannii* and then studied the cell growth in planktonic cultures of *A. baumannii* in the presence of harvested EPS, tobramycin, and Mg^{2+} and Ca^{2+} cations as "blocking agents" for EPS' charged binding sites. When they added these cations together with EPS and tobramycin to the cell culture, they observed a decrease in the bacterial growth rate, suggesting that the protective ability of EPS is compromised, allowing tobramycin to become more effective against the biofilm.[26] This finding, together with the observed increase in the adhesion strengths of bound and loose EPS to the negatively charged Si_3N_4 cantilever in the presence of 10 μg/mL tobramycin, strongly suggests that tobramycin binds to negatively charged groups of EPS by means of an electrostatic interaction,[22] whereas the remaining unbalanced positively charged groups enhance the adhesion to the negatively charged Si_3N_4 AFM cantilever surface. As a result, the tobramycin–EPS interactions would decrease the electrostatic repulsion between EPS and the negatively charged Si_3N_4 AFM cantilever surface and hence increase their adhesion strength.

In addition, in the study of Davenport et al.,[26] both protease-treated and untreated EPS blocked tobramycin's activity, meaning that proteins and DNA did not contribute to EPS protection against tobramycin. Therefore, the negatively charged groups of polysaccharides and other constituents with exceptions of the proteins present in the *A. baumannii* EPS matrix were possibly the main binding agents of tobramycin. Mean mass concentrations of bound and loose EPS showed that the bound EPS contain more carbohydrates than the loose EPS (Table S1). This may partially explain why bound EPS were more susceptible to a high concentration of tobramycin, showing higher adhesion to the negatively charged cantilever, compared to loose EPS. In this context, our results also indicate that introducing tobramycin at either concentration was sufficient to collapse both bound and loose EPS compared to the untreated ones with no change in their mechanics (Table 1). Thus, we conclude that tobramycin acts mainly to change the conformations of the bound and loose EPS molecules when used at low concentrations (Figure S3a,c). However, at higher concentrations, it acts to change both the EPS conformations (Figure S3b,d) as well as the chemical composition of the EPS molecules.

Combined Maltodextrin and Tobramycin Treatment.

Interestingly, the combined treatment of 10 mM maltodextrin with 10 μg/mL tobramycin did not alter substantially the adhesion forces of both bound and loose EPS (Table 1). The distributions of the adhesion forces obtained for the untreated (Figure 3a) and combined-treated EPS (Figure 8a) had similarities. This indicates that the combined treatment had a minimal effect on the chemical compositions of bound and loose EPS. Similarly, no significant change was observed in the frequencies of the adhesion events for both bound and loose EPS (Figure S1). However, when compared with PDs of untreated EPS, the combined treatment resulted in 48% reduction in loose EPS and 22% extension of bound EPS ($P < 0.05$, Table 1). Whereas the collapse in loose EPS was not as significant as when 10 μg/mL tobramycin was used alone, it was the same as when 10 mM maltodextrin was used alone.

Falghoush et al.[37] investigated if a combinatorial treatment of maltodextrin (20, 40, or 60 mM) and tobramycin (50 μg/mL) would reduce the viability of *A. baumannii* cells in biofilms more than when treated with the antibiotic alone. They found that the treatment with maltodextrin alone at all concentrations had no effect on the *A. baumannii* biofilm cell population compared to the untreated ones, but tobramycin alone reduced the logarithm of the colony-forming unit density (cfu/cm^2) by 2.2 log. The combination of tobramycin with 20 mM maltodextrin reduced the cell counts by ~5.5 log. However, when higher maltodextrin concentrations (40 and 60 mM) were combined with tobramycin, the enhanced effect was reversed. Kiamco et al.[36] also reported a similar effect of a combinatorial treatment of maltodextrin (10, 20, or 30 mM) and vancomycin (2 mM) on *S. aureus* biofilms. They reported that vancomycin alone did not effectively reduce the cfu density of *S. aureus* biofilms, even though their data showed a significant statistical difference against the control biofilms. Similarly, when they treated biofilms with maltodextrin alone, they did not observe a relevant reduction of cfu density compared to control biofilms. However, the cfu density was decreased by ~2 log when the biofilm was treated with a combination of 10 mM maltodextrin and 2 mM vancomycin in comparison to the control samples. The use of 20 mM or 30 mM maltodextrin along with 2 mM vancomycin was not effective either.

The observed decrease in the enhanced effect of combinatorial treatment of maltodextrin and antibiotics (tobramycin and vancomycin) at high concentrations could be linked to a reduction in the diffusion of the antibiotic and the treatment effectiveness because of the possible adsorption of maltodextrin on the EPS surface of the biofilms. The above-mentioned reports together with the results of this work suggest that the combined maltodextrin–tobramycin effect could be dose-dependent. As such, when an optimal concentration of the maltodextrin is to be combined with antibiotics, a significant collapse in the EPS molecules, an enhanced effect of the antibiotic on the biofilm, and hence a reduction in biofilm cell counts could be obtained.

Implications toward Control of *A. baumannii* Biofilms.

EPS can potentially contribute to bacterial cells' MDR development through three possible ways. First, the more the adhesive the EPS are, the higher the likelihood it is for biofilms to form with nutrient gradients in the biofilm matrix. These gradients will lead to the formation of bacterial persister cells,[14] which will enhance the MDR. Second, if EPS molecules collapse on the bacterial cell and in the biofilm, then the permeability of the cell wall to nutrients will decrease, resulting in weak biofilms that are susceptible to antibiotics.[77] Third, the EPS collapse may result in embedment of antibiotic diffusion within the biofilm, resulting in enhanced MDR.[78] Note that the effects above are competing in the sense that the more the extended the molecules from the bacterial surface, the higher the expected adhesion.[24,70] On the contrary, more extended molecules indicate less collapse of molecules and as such easier diffusion of antibiotics to the EPS matrix. As such, a sweet spot of a balance between how the collapsed molecules on the bacterial cell impede nutrients' transfer versus how extended they are to facilitate adhesion is what is likely used by the bacterial cells to become MDR.

Our results indicate that applying a hyperosmotic agent such as maltodextrin or NaCl collapses the *A. baumannii* EPS. This collapse is expected to decrease the diffusion of nutrients and oxygen into the biofilm, thus decreasing the growth of the biofilm and its volume. However, such collapse may also limit the diffusion of antibiotics into the biofilm. Even though the diffusion of antibiotics may be limited by the collapsed EPS, we believe that antibiotics could still kill the bacterial cells within the biofilm. In fact, diffusion limitations of nutrients may cause dispersion of the bacterial cells from the biofilm, which is considered as the last stage in a biofilm cycle.[79] Many of the ecological and evolutionary drivers of biofilm dispersal are thought to be slight variations in the environmental quality.[79,80] Therefore, it is not surprising that there is a range of environmental cues that trigger dispersal from the biofilms, including alterations in the availability of nutrients,[77,81,82] oxygen depletion,[83] or low levels of iron.[84] Moreover, the dispersed cells can escape the biofilm EPS matrix by coordinated evacuation from breakup points,[85] leading to the characteristic hollowing of biofilm microcolonies that is observed during the dispersal stage for many biofilms.[79] When the biofilms disperse and planktonic bacterial cells come out of the protective EPS matrix, they will be more susceptible to antibiotics and can be killed easily compared to when they are inside the biofilm matrix. In addition, antibiotics could find their ways to reach the bacterial cells inside the biofilm by passing through the hollows created in the EPS matrix by the dispersed cells.

As such and based on our findings, we suggest that sequential killing of the *A. baumannii* biofilm will first occur when the bacterial cells inside the biofilm are killed by starvation due to nutrients' diffusion limitations and then by antibiotics when the bacterial cells disperse from biofilms. In addition, even if the bacterial cells do not disperse because of limited nutrient diffusion, their growth rate in the biofilm will potentially decrease. This might cause a decrease in the ability of EPS to protect the biofilm because of the degradation of the biofilm matrix and might open ways for antibiotics to diffuse inside the biofilm and kill the bacterial cells. The administration of the antibiotic to kill the viable remaining bacterial cells within the biofilm is expected to be dose-dependent and also varies with the bacterial strain forming the biofilm and causing the infection. Caution should be experienced in generalizing the findings from this study to other bacterial strains. We have previously observed that the adhesion measured between variable strains of *L. monocytogenes* and silicon nitride significantly varied among tested strains.[63,86] As such, we expect variable strains or species to have variable adhesion strengths to the same substrate.[71]

The applicability of the suggested sequential treatment of a hyperosmotic agent followed by an antibiotic remains to be validated on in situ biofilms grown on wounded tissues. In a step toward that, *A. baumannii* biofilms were grown on wounded pig explants extracted from piglet ears for 4 days. The biofilms were then treated with maltodextrin, tobramycin, or a combination of the two. AFM measurements were then performed to quantify the adhesion and the elasticity of the biofilms. A reduced adhesion will indicate that the biofilm structure is jeopardized, and a softer biofilm is expected to facilitate antibiotics' diffusion and as such access to cells within the biofilm, marking efficacy. Indeed, our results (data not shown) indicated that, for example, the combined treatment resulted in 80% less adhesion and 55% softer biofilms compared to untreated samples. As such, even though EPS were not

investigated in their native states (within biofilms), the findings obtained here correlated well with our investigations on biofilms.

CONCLUSIONS

In this work, bound and loose EPS extracted from *A. baumannii* biofilms were used as models to investigate their nanoscale responses to treatments with hyperosmotic agents (NaCl and maltodextrin) combined with or without tobramycin. In the absence of any treatment, it was found that compared to bound EPS, loose EPS were significantly longer in length, and their adhesion to the Si_3N_4 AFM cantilever surface was significantly stronger. Introducing NaCl as a control hyperosmotic agent caused a slight decrease in the adhesion of loose EPS but significantly increased the adhesion of bound EPS. Maltodextrin (1 mM) collapsed significantly both the bound and loose EPS, but 10 mM maltodextrin collapsed only loose EPS. The lengths of bound and loose EPS were significantly extended at the 10 mM maltodextrin compared to when treated with 1 mM maltodextrin, which was likely due to adsorption of maltodextrin on the EPS surfaces. Introducing tobramycin collapsed both bound and loose EPS. The change in the length was independent of the concentration used, but the change in the adhesion was dose-dependent. At a sufficiently higher concentration of tobramycin (10 μg/mL), adhesion of both bound and loose EPS to the AFM cantilever surface significantly increased. The combined treatment of 10 mM maltodextrin with 10 μg/mL tobramycin significantly collapsed only the loose EPS and did not alter the adhesion for both bound and loose EPS to the AFM cantilever surface. In addition, the combined treatment was not as effective as when 10 μg/mL tobramycin was used alone.

Supplementary Material

Refer to Web version on PubMed Central for supplementary material.

ACKNOWLEDGMENTS

Our research was supported by DoD under grant DM110308. We would like to acknowledge Prof. Recep Avci, Director of the Imaging and Chemical Analysis Laboratory (ICAL) at the Montana State University in Bozeman, MT, for utilizing the ToF-SIMS instrument to create micropatterns on silicon surfaces.

REFERENCES

(1). Costerton JW; Stewart PS; Greenberg EP Bacterial biofilms: A common cause of persistent infections. Science 1999, 284, 1318–1322. [PubMed: 10334980]

(2). Asif M; Alvi IA; Rehman SU Insight into *Acinetobacter baumannii*: Pathogenesis, global resistance, mechanisms of resistance, treatment options, and alternative modalities. Infect. Drug Resist. 2018, 11, 1249–1260. [PubMed: 30174448]

(3). Dijkshoorn L; Nemec A; Seifert H An increasing threat in hospitals: Multidrug-resistant *Acinetobacter baumannii*. Nat. Rev. Microbiol. 2007, 5, 939–951. [PubMed: 18007677]

(4). Karageorgopoulos DE; Falagas ME Current control and treatment of multidrug-resistant Acinetobacter baumannii infections. Lancet Infect. Dis. 2008, 8, 751–762. [PubMed: 19022191]

(5). Wong D; Nielsen TB; Bonomo RA; Pantapalangkoo P; Luna B; Spellberg B Clinical and pathophysiological overview of Acinetobacter infections: A century of challenges. Clin. Microbiol. Rev. 2017, 30, 409–447. [PubMed: 27974412]

(6). Teerawattanapong N; Panich P; Kulpokin D; Na Ranong S; Kongpakwattana K; Saksinanon A; Goh B-H; Lee L-H; Apisarnthanarak A; Chaiyakunapruk N A Systematic review of the burden of

multidrug-resistant healthcare-associated infections among intensive care unit patients in Southeast Asia: The rise of multidrug-resistant *Acinetobacter baumannii*. Infect. Control Hosp. Epidemiol. 2018, 39, 525. [PubMed: 29580299]

(7). He X; Lu F; Yuan F; Jiang D; Zhao P; Zhu J; Cheng H; Cao J; Lu G Biofilm formation caused by clinical *Acinetobacter baumannii* isolates is associated with overexpression of the AdeFGH efflux pump. Antimicrob. Agents Chemother. 2015, 59, 4817–4825. [PubMed: 26033730]

(8). Kanafani ZA; Kanj MS Acinetobacter infection: Treatment and prevention. https://www.uptodate.com/contents/acinetobacter-infection-treatment-and-prevention, accessed 2013.

(9). James GA; Swogger E; Wolcott R; Pulcini ED; Secor P; Sestrich J; Costerton JW; Stewart PS Biofilms in chronic wounds. Wound Repair Regen. 2008, 16, 37–44. [PubMed: 18086294]

(10). Lu P-L; Siu LK; Chen TC; Ma L; Chiang WG; Chen YH; Lin SF; Chen TP Methicillin-resistant Staphylococcus aureus and *Acinetobacter baumannii* on computer interface surfaces of hospital wards and association with clinical isolates. BMC Infect. Dis. 2009, 9, 164. [PubMed: 19796381]

(11). Sorci L; Blaby I; De Ingeniis J; Gerdes S; Raffaelli N; Lagard VD; Osterman A Genomics-driven reconstruction of Acinetobacter NAD metabolism: Insights for antibacterial target selection. J. Biol. Chem. 2010, 285, 39490–39499. [PubMed: 20926389]

(12). Dallo SF; Weitao T Insights into Acinetobacter war-wound infections, biofilms, and control. Adv. Skin Wound Care 2010, 23, 169–174. [PubMed: 20299843]

(13). Kaščáková S; Maigre L; Chevalier J; Refregiers M; Pages JM Antibiotic transport in resistant bacteria: Synchrotron UV fluorescence microscopy to determine antibiotic accumulation with single cell resolution. PLoS One 2012, 7, No. e38624.

(14). Fisher RA; Gollan B; Helaine S Persistent bacterial infections and persister cells. Nat. Rev. Microbiol. 2017, 15, 453–464. [PubMed: 28529326]

(15). Sultana ST; Call DR; Beyenal H Eradication of Pseudomonas aeruginosa biofilms and persister cells using an electrochemical scaffold and enhanced antibiotic susceptibility. npj Biofilms Microbiomes 2016, 2, 2. [PubMed: 28649396]

(16). Miyaue S; Suzuki E; Komiyama Y; Kondo Y; Morikawa M; Maeda S Bacterial memory of persisters: Bacterial persister cells can retain their phenotype for days or weeks after withdrawal from colony–biofilm culture. Front. Microbiol. 2018, 9, 1396. [PubMed: 29997606]

(17). Salama Y; Chennaoui M; Sylla A; Mountadar M; Rihani M; Assobhei O Characterization, structure, and function of extracellular polymeric substances (EPS) of microbial biofilm in biological wastewater treatment systems: A review. Desalin. Water Treat. 2016, 57, 16220–16237.

(18). Mah T-FC; O'Toole GA Mechanisms of biofilm resistance to antimicrobial agents. Trends Microbiol. 2001, 9, 34–39. [PubMed: 11166241]

(19). Hall CW; Mah T-F Molecular mechanisms of biofilm-based antibiotic resistance and tolerance in pathogenic bacteria. FEMS Microbiol. Rev. 2017, 41, 276–301. [PubMed: 28369412]

(20). Stewart PS, Antimicrobial tolerance in biofilms. Microbiol. Spectrum 2015, 3, DOI: 10.1128/microbiolspec.mb-0010-2014

(21). Cloete TE Resistance mechanisms of bacteria to antimicrobial compounds. Int. Biodeterior. Biodegrad. 2003, 51, 277–282.

(22). Teirlinck E; Samal SK; Coenye T; Braeckmans K Penetrating the bacterial biofilm: Challenges for antimicrobial treatment In Functionalized Nanomaterials for the Management of Microbial Infection: A Strategy To Address Microbial Drug Resistance; Boukherroub R, Szunerits S, Drider D, Eds.; Elsevier: 2017; pp 49–76.

(23). Abu-Lail NI; Camesano TA Role of ionic strength on the relationship of biopolymer conformation, DLVO contributions, and steric interactions to bioadhesion of *Pseudomonas putida* KT2442. Biomacromolecules 2003, 4, 1000–1012. [PubMed: 12857085]

(24). Abu-Lail NI; Camesano TA Specific and nonspecific interaction forces between Escherichia coli and silicon nitride, determined by Poisson statistical analysis. Langmuir 2006, 22, 7296–7301. [PubMed: 16893229]

(25). Cao B; Shi L; Brown RN; Xiong Y; Fredrickson JK; Romine MF; Marshall MJ; Lipton MS; Beyenal H Extracellular polymeric substances from *Shewanella* sp HRCR-1 biofilms:

Characterization by infrared spectroscopy and proteomics. Environ. Microbiol. 2011, 13, 1018–1031. [PubMed: 21251176]

(26). Davenport EK; Call DR; Beyenal H Differential protection from tobramycin by extracellular polymeric substances from *Acinetobacter baumannii* and Staphylococcus aureus biofilms. Antimicrob. Agents Chemother. 2014, 58, 4755–4761. [PubMed: 24913166]

(27). Wilkinson JF The extracellular polysaccharides of bacteria. Bacteriol. Rev. 1958, 22, 46–73. [PubMed: 13522509]

(28). Tang J; Zhu N; Zhu Y; Kerr P; Wu Y Distinguishing the roles of different extracellular polymeric substance fractions of a periphytic biofilm in defending against Fe_2O_3 nanoparticle toxicity. Environ. Sci.: Nano 2017, 4, 1682–1691.

(29). Guo X; Wang X; Liu JX Composition analysis of fractions of extracellular polymeric substances from an activated sludge culture and identification of dominant forces affecting microbial aggregation. Sci. Rep. 2016, 6, 28391. [PubMed: 27311788]

(30). Hood MI; Jacobs AC; Sayood K; Dunman PM; Skaar EP *Acinetobacter baumannii* increases tolerance to antibiotics in response to monovalent cations. Antimicrob. Agents Chemother. 2010, 54, 1029–1041. [PubMed: 20028819]

(31). van der Waal SV; van der Sluis LWM; Özok AR; Exterkate RAM; van Marle J; Wesselink PR; de Soet JJ The effects of hyperosmosis or high pH on a dual-species biofilm of Enterococcus faecalis and Pseudomonas aeruginosa: An in vitro study. Int. Endod. J. 2011, 44, 1110–1117. [PubMed: 21859433]

(32). Liu C; Niu Y; Zhou X; Zhang K; Cheng L; Li M; Li Y; Wang R; Yang Y; Xu X Hyperosmotic response of Streptococcus mutans: From microscopic physiology to transcriptomic profile. BMC Microbiol. 2013, 13, 275. [PubMed: 24289739]

(33). Dmitrieva NI; Cai Q; Burg MB Cells adapted to high NaCl have many DNA breaks and impaired DNA repair both in cell culture and *in vivo*. Proc. Natl. Acad. Sci. U.S.A. 2004, 101, 2317–2322. [PubMed: 14983007]

(34). Grotz VL; Munro IC An overview of the safety of sucralose. Regul. Toxicol. Pharmacol. 2009, 55, 1–5. [PubMed: 19464334]

(35). Alonso B; Cruces R; Perez A; Fernandez-Cruz A; Guembe M Activity of maltodextrin and vancomycin against staphylococcus aureus biofilm. Front. Biosci., Scholar Ed. 2018, 10, 300–308.

(36). Kiamco MM; Atci E; Khan QF; Mohamed A; Renslow RS; Abu-Lail N; Fransson BA; Call DR; Beyenal H Vancomycin and maltodextrin affect structure and activity of Staphylococcus aureus biofilms. Biotechnol. Bioeng. 2015, 112, 2562–2570. [PubMed: 26084588]

(37). Falghoush A; Beyenal H; Besser TE; Omsland A; Call DR Osmotic compounds enhance antibiotic efficacy against *Acinetobacter baumannii* biofilm communities. Appl. Environ. Microbiol. 2017, 83, No. e01297–17.

(38). Bemis JE; Akhremitchev BB; Walker GC Single polymer chain elongation by atomic force microscopy. Langmuir 1999, 15, 2799–2805.

(39). Bowen WR; Lovitt RW; Wright CJ Application of atomic force microscopy to the study of micromechanical properties of biological materials. J. Biotechnol. Lett. 2000, 22, 893–903.

(40). Li H; Linke WA; Oberhauser AF; Carrion-Vazquez M; Kerkvliet JG; Lu H; Marszalek PE; Fernandez JM Reverse engineering of the giant muscle protein titin. Nature 2002, 418, 998–1002. [PubMed: 12198551]

(41). Clausen-Schaumann H; Rief M; Tolksdorf C; Gaub HE Mechanical stability of single DNA molecules. Biophys. J. 2000, 78, 1997–2007. [PubMed: 10733978]

(42). Abu-Lail NI; Camesano TA Polysaccharide properties probed with AFM. J. Microsc. 2003, 212, 217–238. [PubMed: 14629548]

(43). van der Aa BC; Dufrêne YF In situ characterization of bacterial extracellular polymeric substances by AFM. Colloids Surf., B 2002, 23, 173–182.

(44). Pan M; Zhu L; Chen L; Qiu Y; Wang J Detection techniques for extracellular polymeric substances in biofilms: A review. BioResources 2016, 11, 8092–8115.

(45). Ahimou F; Semmens MJ; Novak PJ; Haugstad G Biofilm cohesiveness measurement using a novel atomic force microscopy methodology. Appl. Environ. Microbiol. 2007, 73, 2897–2904. [PubMed: 17337563]

(46). Wright CJ; Shah MK; Powell LC; Armstrong I Application of AFM from microbial cell to biofilm. Scanning 2010, 32, 134–149. [PubMed: 20648545]

(47). Stuart TL; Mulvey M; Simor AE; Tien HC; Battad A; Taylor G; Vayalumkal JV; Weir C; Ofner M; Gravel D; Paton S *Acinetobacter baumannii* in casualties returning from Afghanistan. Can. J. Infect. Control 2007, 22, 154.

(48). Tien HC; Battad A; Bryce EA; Fuller J; Mulvey M; Bernard K; Brisebois R; Doucet JJ; Rizoli SB; Fowler R; Simor AE Multi-drug resistant *Acinetobacter* infections in critically injured Canadian forces soldiers. *BMC Infect. Dis.* 2007, 7, 95. [PubMed: 17697345]

(49). Kroll A; Behra R; Kaegi R; Sigg L Extracellular polymeric substances (EPS) of freshwater biofilms stabilize and modify CeO_2 and Ag nanoparticles. PLoS One 2014, 9, No. e110709.

(50). Sheng G-P; Yu H-Q; Yu Z Extraction of extracellular polymeric substances from the photosynthetic bacterium *Rhodopseudomonas acidophila*. Appl. Microbiol. Biotechnol. 2005, 67, 125–130. [PubMed: 15309338]

(51). Metzger U; Lankes U; Fischpera K; Frimmel FH The concentration of polysaccharides and proteins in EPS of *Pseudomonas putida* and *Aureobasidum pullulans* as revealed by 13C CPMAS NMR spectroscopy. Appl. Microbiol. Biotechnol. 2009, 85, 197–206. [PubMed: 19795119]

(52). Deliorman M; Wolfenden ML; Suo Z; Beech IB; Yang X; Avci R Immobilization and trapping of living bacteria and applications in corrosion studies In Understanding Biocorrosion: Fundamentals and Applications; Liengen T, Basseguy R, Feron D, Beech IB, Eds.; Woodhead Publishing: Cambridge, UK, 2014; pp 145–165.

(53). Hutter JL; Bechhoefer J Calibration of atomic force microscope tips. Rev. Sci. Instrum. 1993, 64, 1868–1873.

(54). Suo Z; Avci R; Deliorman M; Yang X; Pascual DW Bacteria survive multiple puncturings of their cell walls. Langmuir 2009, 25, 4588–4594. [PubMed: 19260649]

(55). Xie X; Deliorman M; Qasaimeh MA; Percipalle P The relative composition of actin isoforms regulates cell surface biophysical features and cellular behaviors. Biochim. Biophys. Acta, Gen. Subj. 2018, 1862, 1079–1090. [PubMed: 29410074]

(56). Arce FT; Avci R; Beech IB; Cooksey KE; Wigglesworth-Cooksey B A live bioprobe for studying diatomsurface interactions. Biophys. J. 2004, 87, 4284–4297. [PubMed: 15377513]

(57). Abu-Lail NI; Camesano TA The role of lipopolysaccharides in the adhesion, retention, and transport of E. coli JM109. Environ. Sci. Technol. 2003, 37, 2173–83. [PubMed: 12785523]

(58). Fisher TE; Marszalek PE; Oberhauser AF; Carrion-Vazquez M; Fernandez JM The micro-mechanics of single molecules studied with atomic force microscopy. J. Physiol. 2004, 520, 5–14.

(59). Pleshakova T; Bukharina N; Archakov A; Ivanov Y Atomic force microscopy for protein detection and their physicochemical characterization. Int. J. Mol. Sci. 2018, 19, 1142.

(60). Soon RL; Nation RL; Harper M; Adler B; Boyce JD; Tan C-H; Li J; Larson I Effect of colistin exposure and growth phase on the surface properties of live Acinetobacter baumannii cells examined by atomic force microscopy. Int. J. Antimicrob. Agents 2011, 38, 493–501. [PubMed: 21925844]

(61). Gordesli FP; Abu-Lail NI The role of growth temperature in the adhesion and mechanics of pathogenic L. monocytogenes: An AFM study. Langmuir 2012, 28, 1360–1373. [PubMed: 22133148]

(62). Janshoff A; Neitzert M; Oberdorfer Y; Fuchs H Force spectroscopy of molecular systems - Single molecule spectroscopy of polymers and biomolecules. Angew. Chem., Int. Ed. 2000, 39, 3213–3237.

(63). Eskhan AO; Abu-Lail NI Cellular and molecular investigations of the adhesion and mechanics of *Listeria monocytogenes* lineages' I and II environmental and epidemic strains. J. Colloid Interface Sci. 2013, 394, 554–563. [PubMed: 23261349]

(64). Gordesli FP; Abu-Lail NI Impact of ionic strength of growth on the physiochemical properties, structure, and adhesion of Listeria monocytogenes polyelectrolyte brushes to a silicon nitride surface in water. J. Colloid Interface Sci. 2012, 388, 257–267. [PubMed: 23010316]

(65). Abu-Lail NI; Camesano TA Elasticity of *Pseudomonas* putida KT2442 surface polymers probed with single-molecule force microscopy. Langmuir 2002, 18, 4071–4081.

(66). Janissen R; Murillo DM; Niza B; Sahoo PK; Nobrega MM; Cesar CL; Temperini MLA; Carvalho HF; deSouza AA; Cotta MA Spatiotemporal distribution of different extracellualr polymeric substances and filamentation mediate Xylella *fastidiosa* adhesion and biofilm formation. Sci. Rep. 2015, 5, 9856. [PubMed: 25891045]

(67). Buffeteau T; Desbat B; Eyquem D Attenuated total reflection Fourier transform infrared microspectroscopy: Theory and application to polymer samples. Vib. Spectrosc. 1996, 11, 29–36.

(68). Bhargava R Infrared spectroscopic imaging: The next generation. Appl. Spectrosc. 2012, 66, 1091–1120. [PubMed: 23031693]

(69). Tsuneda S; Aikawa H; Hayashi H; Yuasa A; Hirata A Extracellular polymeric substances responsible for bacterial adhesion onto solid surface. FEMS Microbiol. Lett. 2003, 223, 287–292. [PubMed: 12829300]

(70). Camesano TA; Abu-Lail NI Heterogeneity in bacterial surface polysaccharides, probed on a single-molecule basis. Biomacromolecules 2002, 3, 661–667. [PubMed: 12099808]

(71). Park B-J; Abu-Lail NI Atomic force microscopy investigations of heterogeneities in the adhesion energies measured between pathogenic and non-pathogenic *Listeria* species and silicon nitride as they correlate to virulence and adherence. Biofouling 2011, 27, 543–559. [PubMed: 21623482]

(72). Park B-J; Abu-Lail NI The role of the pH conditions of growth on the bioadhesion of individual and lawns of pathogenic *Listeria monocytogenes* cells. J. Colloid Interface Sci. 2011, 358, 611–620. [PubMed: 21459385]

(73). Flemming H-C; Wingender J The biofilm matrix. Nat. Rev. Microbiol. 2010, 8, 623–633. [PubMed: 20676145]

(74). Rahbar MR; Rasooli I; Mousavi Gargari SL; Amani J; Fattahian Y In silico analysis of antibody triggering biofilm associated protein in *Acinetobacter baumannii*. J. Theor. Biol. 2010, 266, 275–290. [PubMed: 20600143]

(75). Brossard KA; Campagnari AA The *Acinetobacter baumannii* biofilm-associated protein plays a role in adherence to human epithelial cells. Infect. Immun. 2012, 80, 228–233. [PubMed: 22083703]

(76). Jiao Y; D'haeseleer P; Dill BD; Shah M; VerBerkmoes NC; Hettich RL; Banfield JF; Thelen MP Identification of biofilm matrix-associated proteins from an acid mine drainage microbial community. Appl. Environ. Microbiol. 2011, 77, 5230–5237. [PubMed: 21685158]

(77). Gjermansen M; Ragas P; Sternberg C; Molin S; Tolker-Nielsen T Characterization of starvation-induced dispersion in *Pseudomonas putida* biofilms. Environ. Microbiol. 2005, 7, 894–904. [PubMed: 15892708]

(78). Anderl JN; Franklin MJ; Stewart PS Role of antibiotic penetration limitation in Klebsiella pneumoniae biofilm resistance to ampicillin and ciprofloxacin. Antimicrob. Agents Chemother. 2000, 44, 1818–1824. [PubMed: 10858336]

(79). McDougald D; Rice SA; Barraud N; Steinberg PD; Kjelleberg S Should we stay or should we go: Mechanisms and ecological consequences for biofilm dispersal. Nat. Rev. Microbiol. 2011, 10, 39–50. [PubMed: 22120588]

(80). Kaplan JB Biofilm dispersal: mechanisms, clinical implications, and potential therapeutic uses. J. Dent. Res. 2010, 89, 205–218. [PubMed: 20139339]

(81). Hunt SM; Werner EM; Huang B; Hamilton MA; Stewart PS Hypothesis for the role of nutrient starvation in biofilm detachment. Appl. Environ. Microbiol. 2004, 70, 7418–7425. [PubMed: 15574944]

(82). Schleheck D; Barraud N; Klebensberger J; Webb JS; McDougald D; Rice SA; Kjelleberg S Pseudomonas aeruginosa PAO1 preferentially grows as aggregates in liquid batch cultures and disperses upon starvation. PLoS Biol. 2009, 4, No. e5513.

(83). An S; Wu J; Zhang L-H Modulation of Pseudomonas aeruginosa biofilm dispersal by a cyclic-di-GMP phosphodiesterase with a putative hypoxia-sensing domain. Appl. Environ. Microbiol. 2010, 76, 8160–8173. [PubMed: 20971871]

(84). Glick R; Gilmour C; Tremblay J; Satanower S; Avidan O; Deziel E; Greenberg EP; Poole K; Banin E Increase in rhamnolipid synthesis under iron-limiting conditions influences surface motility and biofilm formation in Pseudomonas aeruginosa. J. Bacteriol. 2010, 192, 2973–2980. [PubMed: 20154129]

(85). Purevdorj-Gage B; Costerton WJ; Stoodley P Phenotypic differentiation and seeding dispersal in non-mucoid and mucoid Pseudomonas aeruginosa biofilms. Microbiology 2005, 151, 1569–1576. [PubMed: 15870466]

(86). Park B-J; Haines T; Abu-Lail NI A correlation between the virulence and the adhesion of *Listeria monocytogenes* to silicon nitride: An atomic force microscopy study. Colloids Surf., B 2009, 73, 237–243.

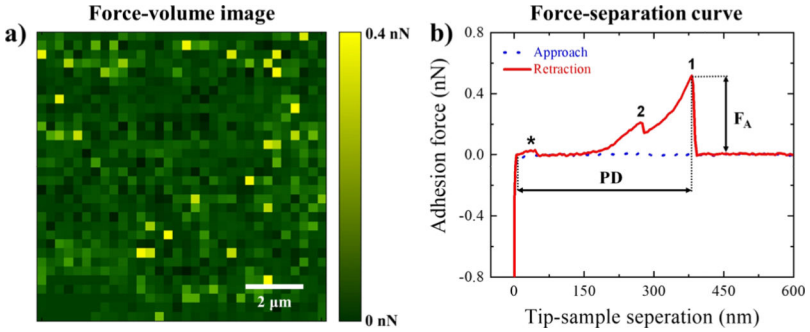

Figure 1.

(a) Example of an FV image and (b) a force–separation curve associated with loose EPS extracted from *A. baumannii* and subsequently immobilized on a silicon wafer surface. Force magnitudes at each pixel in the FV image represent the maximum adhesion forces (F_A) quantified in the retraction force–separation files at that pixel (e.g., peak 1 in the representative retraction curve). The corresponding PDs associated with the biopolymer detachment events were also quantified. While the adhesion forces that possessed values above 0.1 nN cutoff force (e.g., peak 2 in the representative retraction curve) were included in the quantitative analysis, the remaining adhesion events (e.g., peak * in the representative retraction curve) were regarded as noise and excluded from the analysis.

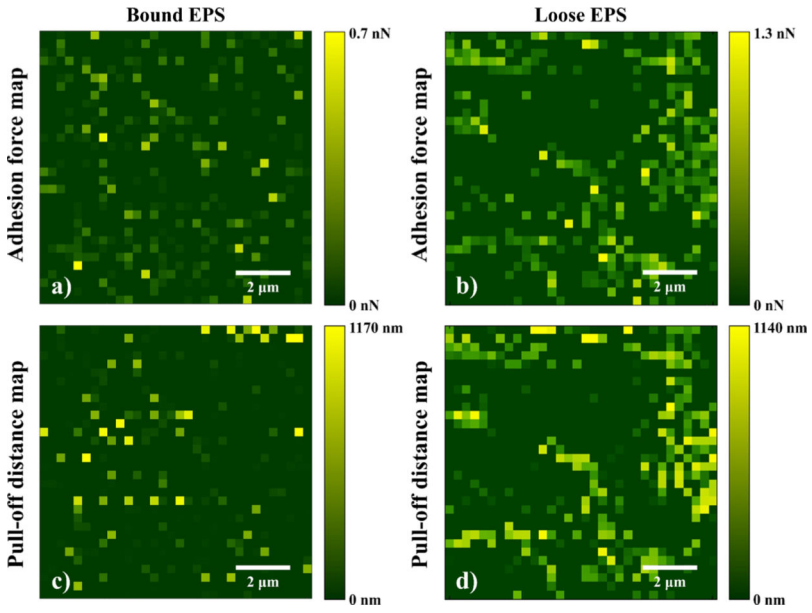

Figure 2.

Representative adhesion force (a,b) and PD maps (b,c) associated with *A. baumannii* untreated bound (a,c) and loose EPS (b,d) immobilized on the silicon wafer surface. Here, maximum adhesion force values (marked with 1 in the retraction curve of Figure 1b) were assigned to each pixel in the adhesion maps, whereas the corresponding PDs were assigned to each pixel in the PD maps. Adhesion and PD values in force profiles with an unclear approach and/or retraction curve were set to 0 at corresponding pixels in the maps.

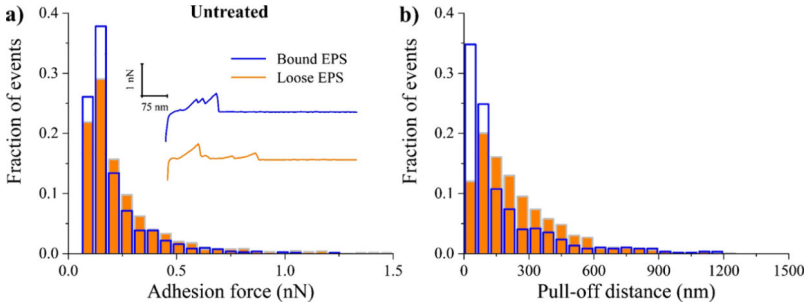

Figure 3.

Distribution histograms of all adhesion force events (a) and PDs (b) collected between *A. baumannii* untreated bound (blue open bars) and loose (orange full bars) EPS in PBS solution ($n = 3$). The inset represents example retraction curves collected on EPS under tested condition.

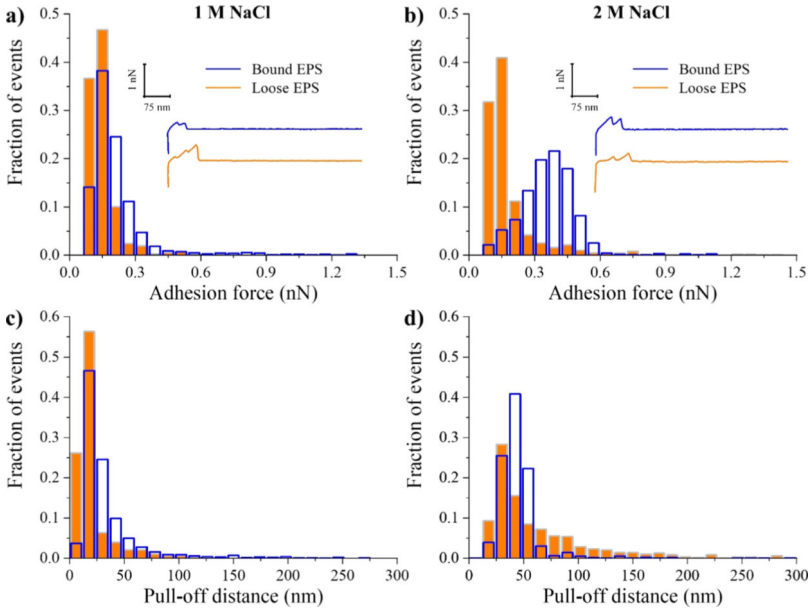

Figure 4.

Distribution histograms of all adhesion force events (a,b) and PDs (c,d) collected between *A. baumannii* bound (blue open bars) and loose (orange full bars) EPS in solutions of 1 and 2 M NaCl (control), respectively ($n = 3$). The insets represent example retraction curves collected on EPS under tested conditions.

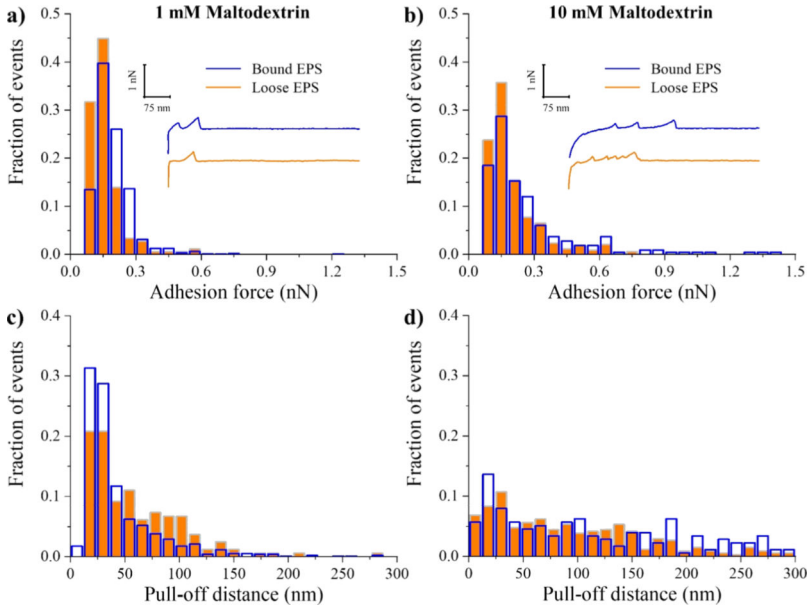

Figure 5.

Distribution histograms of all adhesion force events (a,b) and PDs (c,d) collected between *A. baumannii* bound (blue open bars) and loose (orange full bars) EPS in solutions of 1 and 10 mM maltodextrin, respectively ($n = 3$). The insets represent example retraction curves collected on EPS under tested conditions.

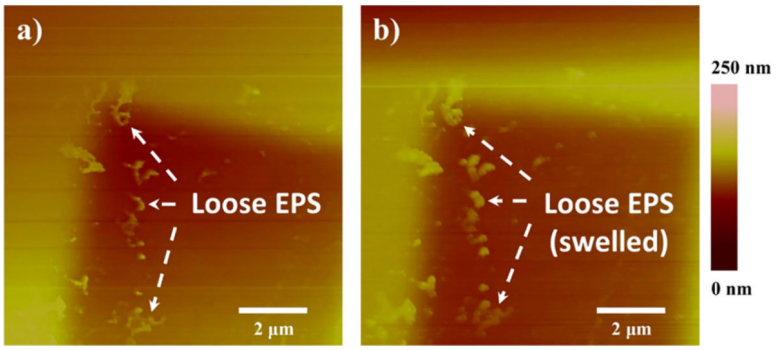

Figure 6.

AFM height images of *A. baumannii* loose EPS (bright futures in the images pointed by arrows) immobilized on predefined areas of the silicon wafer surface before (a) and after (b) exposure to 10 mM maltodextrin. Both images were taken in liquid using the contact mode. The EPS swell after exposure to chemical stress, confirming the conformational changes of biopolymers on the substrate surface.

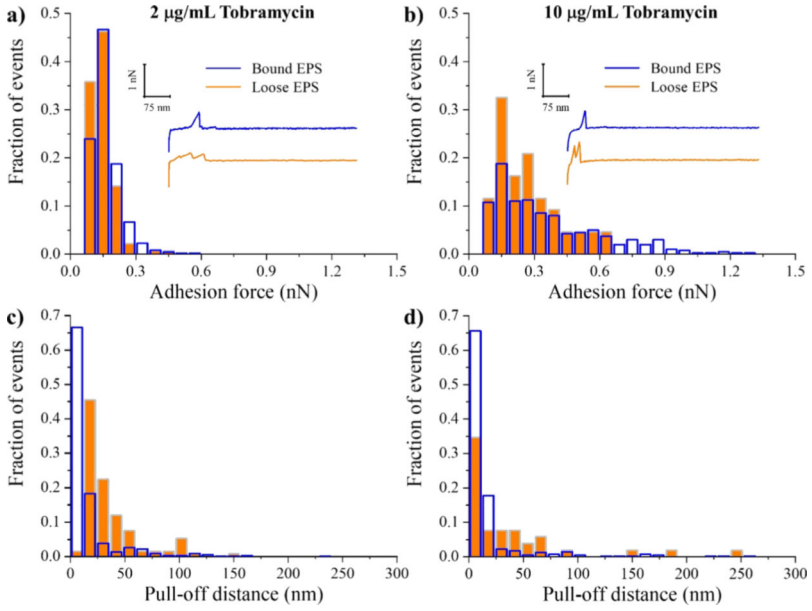

Figure 7.

Distribution histograms of all adhesion force events (a,b) and PDs (c,d) collected between *A. baumannii* bound (blue open bars) and loose (orange full bars) EPS in solutions of 2 and 10 μg/mL tobramycin, respectively (n = 3). The insets represent example retraction curves collected on EPS under tested conditions.

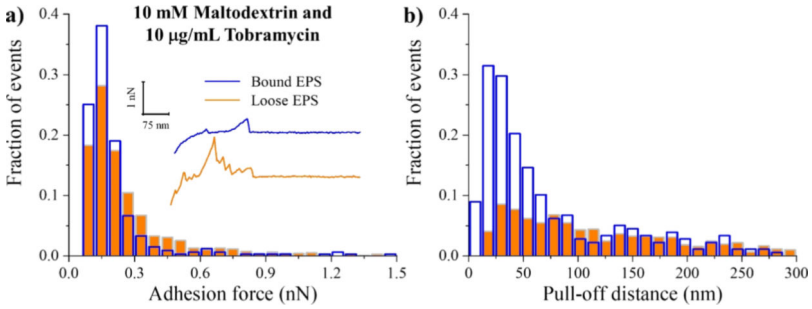

Figure 8.

Distribution histograms of all adhesion force events (a) and PDs (b) collected between *A. baumannii* bound (blue open bars) and loose (orange full bars) EPS in a combined solution of 10 mM maltodextrin and 10 μg/mL tobramycin (n = 3). The inset represents example retraction curves collected on EPS under tested condition.

Table 1.

Summary of AFM Adhesion Force, F_A, and PD, Measurements for *A. baumannii* Bound and Loose EPS

	bound EPS			loose EPS		
condition[a]	**F_A (nN)**	**PD (nm)**	**no. of events**	**F_A (nN)**	**PD (nm)**	**no. of events**
untreated	0.144 ± 0.002	106.4 ± 4.7	828	0.177 ± 0.002	218.0 ± 9.2	1677
			NaCl			
1 M	0.172 ± 0.001	26.1 ± 5.9	1569	0.129 ± 0.001	15.9 ± 0.2	368
2 M	0.378 ± 0.007	28.3 ± 3.4	1149	0.135 ± 0.001	48.6 ± 0.5	830
			Maltodextrin			
1 mM	0.175 ± 0.001	41.7 ± 0.2	964	0.138 ± 0.001	40.8 ± 4.0	501
10 mM	0.172 ± 0.004	177.6 ± 13.2	216	0.152 ± 0.003	112.1 ± 5.7	336
			Tobramycin			
2 μg/mL	0.149 ± 0.001	28.8 ± 7.2	480	0.136 ± 0.001	22.1 ± 0.8	134
10 μg /mL	0.275 ± 0.026	28.4 ± 0.3	399	0.205 ± 0.022	17.8 ± 9.6	52
combined[b]	0.151 ± 0.001	137.0 ± 6.7	331	0.174 ± 0.003	113.1 ± 7.1	933

[a] *A. baumannii* bound and loose EPS were investigated either untreated or in the presence of different concentrations of NaCl, maltodextrin, and tobramycin solutions in PBS, as indicated in the table.

[b] Applied combined concentrations were 10 mM maltodextrin and 10 μg/mL tobramycin, both dissolved in PBS. Peak values and standard deviations were derived from distribution histograms by using the lognormal probability density function. For each set of experiment, 1024 pairs of force versus displacement curves were acquired from three different areas in the FV mode. Data represents mean ± S.D.